Technical information supporting the 2023 Urban heat environmental trend and condition report card

Department for Environment and Water
August, 2023

DEW Technical note 2023/57

Government of South Australia
Department for Environment and Water

Department for Environment and Water

Government of South Australia

August 2023

81-95 Waymouth St, ADELAIDE SA 5000

Telephone +61 (8) 8463 6946

Facsimile +61 (8) 8463 6999

ABN 36702093234

www.environment.sa.gov.au

Disclaimer

The Department for Environment and Water and its employees do not warrant or make any representation regarding the use, or results of the use, of the information contained herein as regards to its correctness, accuracy, reliability, currency or otherwise. The Department for Environment and Water and its employees expressly disclaims all liability or responsibility to any person using the information or advice. Information contained in this document is correct at the time of writing.

Preferred way to cite this publication

Department for Environment and Water (2023). *Technical information supporting the 2023 Urban heat environmental trend and condition report card*, DEW Technical report 2023/57, Government of South Australia, Department for Environment and Water, Adelaide.

Download this document at https://data.environment.sa.gov.au

Acknowledgement of Country

We acknowledge and respect the Traditional Custodians whose ancestral lands we live and work upon and we pay our respects to their Elders past and present. We acknowledge and respect their deep spiritual connection and the relationship that Aboriginal and Torres Strait Islanders people have to Country. We also pay our respects to the cultural authority of Aboriginal and Torres Strait Islander people and their nations in South Australia, as well as those across Australia.

Acknowledgements

This document was prepared by Blair Pellegrino, James Peters and Sarah White (DEW). Matthew Miles (DEW) provided principal oversight throughout and technical review of this report. David Hart provided external technical review of this report and underlying methodologies. Brady Stead (DEW) provided mapping support. Improvements were made to this report and associated report card based on reviews by Amy Ide (DEW) and Louisa Halliday (DEW).

Contents

List of figures

List of tables

Summary

The 2023 release of South Australia's environmental trend and condition report cards summarises our understanding of the current condition of the South Australian environment, and how it is changing over time.

This document describes the indicators, information sources, analysis methods and results used to develop this report and the associated 2023 Urban heat report card. The reliability of information sources used in the report card is also described.

The Urban heat report card sits within the report card Liveability theme and Urban sub-theme. Report cards are published by the Department for Environment and Water and can be accessed at www.environment.sa.gov.au.

1 Introduction

1.1 Environmental trend and condition reporting in SA

The Minister for Climate, Environment and Water under the *Landscape South Australia Act 2019* is required to 'monitor, evaluate and audit the state and condition of the State's natural resources, coasts and seas; and to report on the state and condition of the State's natural resources, coasts and seas' (9(1(a-b)). Environmental trend and condition report cards are produced as the primary means for the Minister to undertake this reporting. Trend and condition report cards are also a key input into the State of the Environment Report for South Australia, which must be prepared under the *Environment Protection Act 1993*. This Act states that the State of the Environment Report must:

- include an assessment of the condition of the major environmental resources of South Australia (112(3(a))), and
- include a specific assessment of the state of the River Murray, especially taking into account the Objectives for a Healthy River Murray under the *River Murray Act 2003* (112(3(ab))), and
- identify significant trends in environmental quality based on an analysis of indicators of environmental quality (112(3(b))).

1.2 Purpose and benefits of SA's trend and condition report cards

South Australia's environmental trend and condition report cards focus on the state's priority environmental assets and the pressures that impact on these assets. The report cards present information on trend, condition, and information reliability in a succinct visual summary.

The full suite of report cards captures patterns in trend and condition, generally at a state scale, and gives insight to changes in a particular asset over time. They also highlight gaps in our knowledge on priority assets that prevent us from assessing trend and condition and might impede our ability to make evidence-based decisions.

Although both trend and condition are considered important, the report cards give particular emphasis to trend. Trend shows how the environment has responded to past drivers, decisions, and actions, and is what we seek to influence through future decisions and actions.

The benefits of trend and condition report cards include to:

- provide insight into our environment by tracking its change over time
- interpret complex information in a simple and accessible format
- provide a transparent and open evidence base for decision-making
- provide consistent messages on the trend and condition of the environment in South Australia
- highlight critical knowledge gaps in our understanding of South Australia's environment
- support alignment of environmental reporting, ensuring we 'do once, use many times'.

Environmental trend and condition report cards are designed to align with and inform state of the environment reporting at both the South Australian and national level. The format, design and accessibly of the report cards has been reviewed and improved with each release.

1.3 Urban heat

As part of the assessment of the major environmental resources of South Australia, this technical report and associated report card will assess the trend and condition of urban heat across metropolitan Adelaide.

Urban heat refers to higher temperatures, relative to non-urban areas which can negatively impact the health and wellbeing of people and communities. Urban heat accumulates in built up (urban) areas because they contain a higher proportion of building materials and heat retaining surfaces, such as bricks, roads, carparks and concrete, compared to natural environments. These surfaces tend to absorb and store heat (mostly from the sun) and then radiate this heat back out into the surrounding area (Wai et al. 2022). These materials can continue releasing heat after air temperatures have cooled, leading to higher evening temperatures in urban areas and exacerbating cumulative impacts of heat waves (Norton et al. 2015).

Urban areas also typically have less vegetation compared to rural areas. Vegetation helps to naturally cool surrounding areas by shading building surfaces, blocking radiation from the sun, and releasing moisture into the atmosphere through evapotranspiration (Bartesaghi-Koc et al. 2022). Water also provides natural cooling, however urban surfaces such as roads cause rainfall to run off quickly, reducing the amount that can be absorbed by the landscape (Adapt NSW 2023).

As heatwaves increase in frequency, intensity and duration due to climate change, impacts will be exacerbated disproportionally in cities due to the increased accumulation of heat in urban areas (Shukla et al. 2019). Analysis undertaken by the Physical Environment Research Network (2021) found that, between 1950 and 2011, Adelaide experienced the greatest increase in average heatwave intensity (2.5 °C) and the greatest increase in the average peak heatwave intensity (4.5 °C) of Australia's capital cities. During heatwaves between 2010 and 2017, Adelaide was also the capital city with the greatest increase in mortality and excess deaths related to heatwaves (8%) (Physical Environment Research Network 2021). If these trends continue into the future, Adelaide is the Australian capital city most at risk of heat related death or illness. High temperatures impact most severely on communities with low socioeconomic status (Bartesaghi-Koc et al. 2022). These communities are less able to escape or mitigate the effects of urban heat through less access to open public green spaces, cost of air-conditioning, working manual, outdoor jobs, or language barriers inhibiting access to support and health care services.

1.4 Measuring urban heat

Urban heat can be quantified either by measuring the temperature of the air, or the temperature of surfaces.

Air temperature can be considered either in terms of the canopy layer, which ranges from ground level to tree canopy height, or the boundary layer, which extends into the atmosphere above canopy height (Zhou et al. 2019). The former is typically measured using in-situ sensors such as those mounted in meteorological stations or alternatively using sensors mounted to vehicles, while the latter can be measured by sensors mounted to tall towers, weather balloons or aircraft (Voogt 2008). Surface temperature on the other hand is typically measured using remotely sensed data, either satellite imagery or airborne imagery (Voogt 2008).

Despite the stronger connection between air temperature and human thermal comfort, most cities including Adelaide lack a network of in-situ sensors which would allow air urban heat to be measured and tracked over time. Therefore surface temperature is often used in studies to assess urban heat (Zhou et al. 2019).

Remote sensing represents a spatially explicit approach to measuring urban heat, and satellite imagery in particular ensures these measurements are spatially, temporally and spectrally consistent. Despite some limitations, such as the impact of cloud, the need for accurate atmospheric corrections and the inherent challenge of assigning a single temperature value to a pixel containing a heterogeneous (and therefore thermally diverse) urban landscape, satellite imagery is widely used in urban heat studies (Zhou et al. 2019).

Three general approaches currently exist for using surface temperature to measure urban heat (Zhou et al. 2019):

1. Using land surface temperature to differentiate areas of higher temperatures relative to other areas in the landscape
2. Calculating the difference in surface temperature between urban areas and surrounding reference areas, to determine the intensity of urban heat
3. Using statistical models to calculate the intensity of urban heat.

While the first option represents a relatively simple method and is useful for investigating patterns of urban heat and the relationship between surface temperature and land covers, it is not well suited to assessing temporal trends due to the impact of varying weather conditions on the day of capture. For this reason, it was not pursued for this report card.

The second option, adopted for this report card, is much better suited to assessing temporal trends as well as comparing urban heat across multiple cities since it employs a relative measure of urban heat (i.e. intensity) rather than an absolute measure. The greatest limitation of this approach is the uncertainty associated with defining urban and reference areas, and the subsequent difficulty in quantifying reference temperatures across highly modified landscapes.

While the final option overcomes this limitation by relying on statistical models, it is a relatively new method and has only been applied in a few studies to date, therefore was not pursued for this report card.

2 Methods

2.1 Indicator

The indicator used for the urban heat report card is urban heat intensity. Urban heat intensity measures the extent to which an urban area experiences temperatures greater than an equivalent reference area without any urban development. This measure seeks to account for any underlying temperature trends within the study area, such as those driven by factors such as elevation, latitude or proximity to the coast and therefore quantify the additional heat in the landscape which is directly attributable to urban development.

2.2 Data sources

The following data sources were used in this report card analysis:

- Landsat 8 and 9 satellite imagery (U.S. Geological Survey (USGS))
- SA land cover data for the 2015–2020 time period (DEW)
- Local government areas (Department for Trade and Investment (DTI))
- Australian Climate Observation Reference Network – Surface Air Temperature (ACORN-SAT) (Bureau of Meteorology (BOM)).

2.3 Data collection

Thermal imagery from the Landsat satellite was downloaded from Earth Explorer (https://earthexplorer.usgs.gov/) for the path/row 097/084, which covers the entire metropolitan Adelaide study area. Downloaded imagery had already been processed to level 2 to ensure both geometric and radiometric corrections had been applied and it was analysis ready. To minimise any potential impact of sensor differences, only Landsat 8 and 9 imagery was used in this analysis. Both these Landsat missions carry the same Thermal Infrared Sensor (TIRS) instrument, which captures thermal data between 10.6–11.19 µm (band 10) and 10.5–12.51 µm (band 11) at 100 m resolution (resampled to 30 m).

The analysis included imagery acquired between December 2013 and January 2023. The start date was chosen to coincide with the availability of Landsat 8 data, which was launched in February 2013 and became operational in April 2013. The end date coincides with the data available at the time of undertaking the analysis. Only imagery from the summer months of December, January and February was used in the analysis, to align with the hottest months when the impact of urban heat is at its greatest, and to reduce any seasonal fluctuations in temperature throughout the year. Any imagery containing cloud or smoke within the study area was excluded.

A total of 25 Landsat images met these criteria and were used in this analysis (Table 2.1). Each summer includes between 1 and 5 images. The corresponding maximum temperatures based on BOM's ACORN-SAT data are also provided in Table 2.1 and were used to confirm that urban heat intensity was not correlated to maximum temperature.

Table 2.1. List of Landsat images included in analysis

Year	Landsat product identifier	Landsat mission	Acquisition date	Maximum temperature (°C)*
2013–14	LC08_L2SP_097084_20131216_20200912_02_T1	Landsat 8	16/12/2013	29.0
2014–15	LC08_L2SP_097084_20141203_20200910_02_T1	Landsat 8	3/12/2014	31.5
	LC08_L2SP_097084_20150205_20200909_02_T1	Landsat 8	5/02/2015	28.4
2015–16	LC08_L2SP_097084_20151222_20200908_02_T1	Landsat 8	22/12/2015	30.7
	LC08_L2SP_097084_20160107_20200907_02_T1	Landsat 8	7/01/2016	30.3
	LC08_L2SP_097084_20160208_20200907_02_T1	Landsat 8	8/02/2016	28.3
2016–17	LC08_L2SP_097084_20161224_20200905_02_T1	Landsat 8	24/12/2016	34.7
	LC08_L2SP_097084_20170125_20200905_02_T1	Landsat 8	25/01/2017	26.6
	LC08_L2SP_097084_20170210_20200905_02_T1	Landsat 8	10/02/2017	38.5
	LC08_L2SP_097084_20170226_20200905_02_T1	Landsat 8	26/02/2017	26.0
2017–18	LC08_L2SP_097084_20171211_20200902_02_T1	Landsat 8	11/12/2017	28.8
	LC08_L2SP_097084_20180213_20200902_02_T1	Landsat 8	13/02/2018	28.9
2018–19	LC08_L2SP_097084_20190216_20200829_02_T1	Landsat 8	16/02/2019	30.1
2019–20	LC08_L2SP_097084_20200102_20200823_02_T1	Landsat 8	2/01/2020	31.8
2020–21	LC08_L2SP_097084_20201203_20210313_02_T1	Landsat 8	3/12/2020	28.8
2021–22	LC08_L2SP_097084_20211206_20211215_02_T1	Landsat 8	6/12/2021	25.8
	LC08_L2SP_097084_20211222_20211230_02_T1	Landsat 8	22/12/2021	29.7
	LC09_L2SP_097084_20211230_20220121_02_T1	Landsat 9	30/12/2021	37.6
	LC09_L2SP_097084_20220115_20220225_02_T1	Landsat 9	15/01/2022	26.7
	LC08_L2SP_097084_20220224_20220303_02_T1	Landsat 8	24/02/2022	33.2
2022–23	LC09_L2SP_097084_20221201_20221203_02_T1	Landsat 9	1/12/2022	26.1
	LC09_L2SP_097084_20221217_20221223_02_T1	Landsat 9	17/12/2022	27.7
	LC08_L2SP_097084_20221225_20230103_02_T1	Landsat 8	25/12/2022	32.9
	LC08_L2SP_097084_20230110_20230124_02_T1	Landsat 8	10/01/2023	31.9
	LC09_L2SP_097084_20230219_20230221_02_T1	Landsat 9	19/01/2023	29.7

* Maximum temperatures from 2013 to 2021 are based on BOM's ACORN-SAT data to account for the shift in Adelaide's primary weather station from Kent Town (station number 023090) to West Terrace (station number 23000) in 2017. ACORN-SAT data was unavailable from 2022 onwards, therefore these temperatures are based on the maximum recorded temperature at West Terrace.

2.4 Data analysis

Study area

The study area defined for this analysis includes 18 local government areas (LGAs) across the metropolitan Adelaide region (Figure 2.1). All data analysis was restricted to the extent of the study area.

Land surface temperature

The thermal bands of Landsat imagery processed to level-2 have already been converted from top-of-atmosphere brightness temperature to surface temperature in degrees Kelvin, and undergone emissivity corrections using Advanced Spaceborne Thermal Emission and Reflection Radiometer (ASTER) Global Emissivity Dataset (GED) and ASTER Normalised Difference Vegetation Index (NDVI) data based on the single channel algorithm (USGS 2022). Further details about this pre-processing can be found in USGS (2021).

Land surface temperature (LST) was calculated by converting band 10 pixel values from degrees Kelvin to degrees Celsius using the following equation:

$$LST_{Celsius} = \left((B10 \times B10_{mult}) + B10_{add}\right) - 273.15$$

where $LST_{Celsius}$ is the land surface temperature in degrees Celsius, $B10$ is the band 10 digital number, $B10_{mult}$ is the band 10 multiplier value (i.e. 0.00341802 for Landsat 8 and 9) and $B10_{add}$ is the band 10 additive value (i.e. 149 for Landsat 8 and 9).

This was repeated for all images in the analysis.

Figure 2.1. Study area showing the 18 LGAs and reference areas

Reference areas

In order to calculate urban heat intensity, reference areas within the study area must first be defined. Reference areas in other studies vary, but can include native vegetation, forests, water bodies, croplands, rural areas and other low intensity impervious surfaces (Zhou et al. 2019).

Reference areas in this analysis were defined as areas of woody native vegetation, as mapped in the SA land cover dataset for the 2015–2020 time period. It was assumed than any areas mapped as woody native vegetation in this dataset were woody native vegetation throughout the entire study period.

Other native vegetation classes such as mangroves, saltmarsh and wetlands, and non-native vegetation such as agriculture, orchards and vineyards were excluded since they weren't considered to be thermally representative of the broader study area prior to urbanisation. Areas mapped as plantation were also excluded due to the potential for these land cover types to change dramatically over the study period.

All reference areas were internally buffered by 100 m to reduce any edge effects from the surrounding urban landscape. The final reference areas are shown in Figure 2.1.

Reference LST

A sample of 1000 random points (with a minimum 100 m spacing) was taken within the reference areas. LST values were extracted at each random point and then used to generate a linear trend of reference LSTs across the study area. This linear trend is the basis of the correction applied to LST to account for any broad-scale temperature trends across the study area, such as those driven by factors such as elevation and proximity to the coast. This was repeated for all images in the analysis.

This approach of determining a linear trend for reference LSTs across the study area is consistent with the approach taken by Devereaux and Caccetta (2017). Ideally, the reference areas would be representatively distributed across the study area, however much of the remaining large stands of native woody vegetation in Adelaide are restricted to the Mount Lofty Ranges and foothills. The northern and western areas of the study area are not well represented, therefore it is expected that the reference LSTs in these areas are less accurate than the southern and eastern areas. This is a limitation of the geography of Adelaide when attempting to fit a simple linear trend based on limited and poorly distributed reference areas.

Urban heat intensity

For each image in the time period, the difference between the LST and the reference LST was calculated to determine the urban heat intensity and therefore quantify the additional heat in the landscape which is attributable to urban development.

Calculating trend

For this analysis, trend represents the change in urban heat intensity over the period from the summer of 2013–14 to the summer of 2022–23.

All urban heat intensity images in the time period were added to a multidimensional raster dataset before calculating a temporal linear trend for each pixel in the study area. This trend was used to fit values for 1 January 2014 (i.e. the first summer in the time period) and 1 January 2023 (i.e. the last summer in the time period) for all pixels in the study area. The difference between these temperatures was used to calculate the change in urban heat intensity over the time period, where a positive value indicates an increase in urban heat intensity (i.e. warming) and a negative value indicates a decrease in urban heat intensity (i.e. cooling). This approach of determining a temporal linear trend for each pixel in the study area is consistent with the approach taken by Kovacs-Ledo and Archibald (2022) (see also Appendix A).

Zonal statistics were used to calculate the average change in urban heat intensity for the entire study area, as well as for each LGA. Standard deviation was also calculated to estimate the spread of values.

Calculating condition

For this analysis, condition represents the urban heat intensity for the summer of 2022–23 (i.e. at the time this analysis was undertaken).

Condition was based on fitting the temporal linear trend for 1 January 2023 (i.e. the last summer of the time period) for each pixel in the study area to estimate the urban heat intensity at the end of the time period. Positive values indicate an area is warmer than expected compared to an equivalent reference area without any urban development, while negative values indicate an area is cooler than expected compared to an equivalent reference area without any urban development.

Zonal statistics were used to calculate the average urban heat intensity for the entire study area, as well as for each LGA. Standard deviation was also calculated to estimate the spread of values.

2.5 Methods to assign trend, condition and reliability

2.5.1 Trend

The method used to calculate urban heat intensity contains some inherent variability as a result of the location of the random points used to generate the reference LST. That is to say, there will be slight variations in the resultant reference LST depending on the location of the random points.

Based on trials where different random points were generated, it was estimated that impacts on the trend results at the study area and LGA scale were minimal (i.e. in the order of 0.2 °C). Therefore a threshold of ±0.5 °C was chosen to indicate no change (Table 2.2).

Table 2.2. Definition of trend classes used

Trend	Description	Threshold
Getting better	Over a scale relevant to tracking change in the indicator it is improving in status with good confidence	≥0.5 °C decrease
Stable	Over a scale relevant to tracking change in the indicator it is neither improving nor declining in status	< ±0.5 °C change
Getting worse	Over a scale relevant to tracking change in the indicator it is declining in status with good confidence	≥0.5 °C increase
Unknown	Data are not available, or are not available at relevant temporal scales, to determine any trend in the status of this resource	-
Not applicable	This indicator of the natural resource does not lend itself to being classified into one of the above trend classes	-

2.5.2 Condition

Assigning condition thresholds to urban heat intensity is challenging and there are no agreed thresholds defined either by the literature or by local, state or national policies. Urban heat intensity can vary based on location, climate, time of year and the reference areas selected in the study, and as a result, studies have applied different thresholds based on their specific requirements and circumstances (Jain et al. 2020).

Condition classes assigned for this analysis (Table 2.3) were based on the range of intensity values observed for this analysis (Table 2.3). Since this is the first analysis assessing urban heat intensity for Adelaide and the first time this report card has been produced, it is recommended these thresholds are reviewed in the future to ensure they remain suitable.

Table 2.3. Definition of condition classes used

Condition	Description	Threshold
Very good	The natural resource is in a state that meets all environmental, economic and social expectations, based on this indicator. Thus, desirable function can be expected for all processes/services expected of this resource, now and into the future, even during times of stress (e.g. prolonged drought)	≤1 °C
Good	The natural resource is in a state that meets most environmental, economic and social expectations, based on this indicator. Thus, desirable function can be expected for only some processes/services expected of this resource, now and into the future, even during times of stress (e.g. prolonged drought)	>1-2 °C
Fair	The natural resource is in a state that does not meet some environmental, economic and social expectations, based on this indicator. Thus, desirable function cannot be expected from many processes/services expected of this resource, now and into the future, particularly during times of stress (e.g. prolonged drought)	>2-4 °C
Poor	The natural resource is in a state that does not meet most environmental, economic and social expectations, based on this indicator. Thus, desirable function cannot be expected from most processes/services expected of this resource, now and into the future, particularly during times of stress (e.g. prolonged drought)	>4 °C
Unknown	Data are not available to determine the state of this natural resource, based on this indicator	-
Not applicable	This indicator of the natural resource does not lend itself to being classified into one of the above condition classes	-

2.5.3 Reliability

Information is scored for reliability based on the minimum of subjective scores (1 [worst] to 5 [best]) given for information currency, applicability, level of spatial representation and accuracy. Definitions guiding the application of these scores are provided in Table 2.4 for currency, Table 2.5 for applicability, Table 2.6 for spatial representation and Table 2.7 for accuracy.

Table 2.4. Guides for applying information currency

Currency score	Criteria
1	Most recent information >10 years old
2	Most recent information up to 10 years old
3	Most recent information up to 7 years old
4	Most recent information up to 5 years old
5	Most recent information up to 3 years old

Table 2.5. Guides for applying information applicability

Applicability score	Criteria
1	Data are based on expert opinion of the measure
2	All data based on indirect indicators of the measure
3	Most data based on indirect indicators of the measure
4	Most data based on direct indicators of the measure
5	All data based on direct indicators of the measure

Table 2.6. Guides for applying spatial representation of information (sampling design)

Spatial score	Criteria
1	From an area that represents less than 5% the spatial distribution of the asset within the region/state or spatial representation unknown
2	From an area that represents less than 25% the spatial distribution of the asset within the region/state
3	From an area that represents less than half the spatial distribution of the asset within the region/state
4	From across the whole region/state (or whole distribution of asset within the region/state) using a sampling design that is not stratified
5	From across the whole region/state (or whole distribution of asset within the region/state) using a stratified sampling design

Table 2.7. Guides for applying accuracy information

Accuracy score	Criteria
1	Better than could be expected by chance
2	> 60% better than could be expected by chance
3	> 70 % better than could be expected by chance
4	> 80 % better than could be expected by chance
5	> 90 % better than could be expected by chance

2.6 Data transparency

Data transparency for this report card is represented in Appendix B.

3 Results

3.1 Trend

Across the entire study area, the average urban heat intensity has increased by 0.2 °C from 1 January 2014 to 1 January 2023, indicating an overall stable trend.

Over the analysed period, urban heat intensity varied between 1.1 °C on 10 February 2017 and 4.8 °C on 13 February 2018. As shown in Figure 3.1, the urban heat intensity fluctuated depending on the date of the image, which reinforces the rationale for using as many images as possible to generate a more robust and representative trend. The average maximum daily temperature over the same period was 30.1 °C, and varied between 25.8 °C on 6 December 2021 and 38.5 °C on 10 February 2017. There was no correlation between urban heat intensity across Adelaide and the maximum daily temperature recorded by BOM.

While the results indicate an overall stable trend, there is significant variation at the local scale within the study area showing areas of both warming and cooling since 2014 (Figure 3.2). For example, there is a significant warming visible over the Dry Creek salt fields, where ponds have dried over this time period due to closure of salt mining operations. Conversely, some ponds north in St Kilda show a cooling trend, due to being full at the end of the time period after previously being dry.

Other examples of significant warming include:

- Replacement of natural turf sporting fields with artificial turf in Woodville South, Klemzig, Wynn Vale, Ridgehaven and Regency Park
- Loss of vegetation cover at Victoria Park in Adelaide
- Loss of established housing and vegetation cover in favour of new developments and urban infill in Felixstow and Campbelltown
- Demolition of the Le Cornu building in Forestville
- Removal of shade structures over car storage yards in Outer Harbor
- Replacement of plantations and other vegetation with solar panels in Happy Valley and Hope Valley
- Addition of solar panels to industrial and commercial buildings in Thebarton and Lockleys
- Construction of industrial sheds in Regency Park, Gillman and Lonsdale; note that these were often constructed several years prior to the beginning of the study however significant warming was still observed during the study period
- Loss of vegetation cover around the Mount Bold reservoir following the Cherry Gardens bushfire
- Changes to irrigation and agricultural practices in Virginia.

Other examples of significant cooling include:

- Establishment of irrigated sporting fields in West Beach
- Construction of cool white roofed industrial buildings in Adelaide Airport, Beverley, Woodville, Gepps Cross, Dudley Park and Edwardstown
- Transition of bare undeveloped land to residential developments in Lightsview

- Creation of artificial wetlands, parklands and recreation reserves in Felixstow, Golden Grove and Adelaide
- Increase in irrigation in the Adelaide parklands
- Recovery of vegetation following the Sampson Flat bushfire
- Gradual restoration and changes to land management practices at Glenthorne farm, now Glenthorne National Park-Ityamaiitpinna Yarta, in O'Halloran Hill
- Changes to irrigation and agricultural practices in Virginia.

These areas of significant warming and cooling are typically larger homogenous areas better detected by the resolution of the Landsat imagery (100 m resolution). Changes at this scale are strongly driven by broadscale land use changes, and will be particularly influenced if these land use changes coincide with either the start or end of the time period analysed. For example, the cooling effect observed in the Lightsview development is restricted to those areas which are bare undeveloped land at the beginning of the time period, rather than those areas where development had already commenced.

While additional changes are likely to be occurring at a finer scale, such as from loss and planting of individual trees, the resolution of the imagery is less able to detect these changes, particularly when occurring within a heterogeneous landscape.

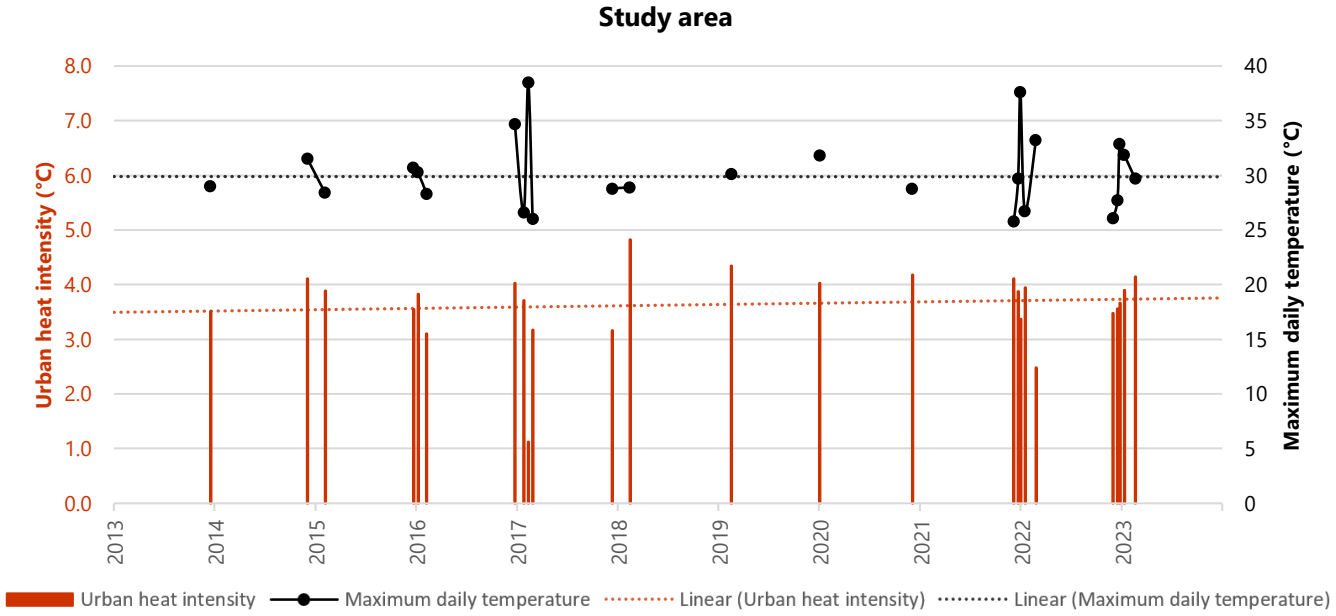

Figure 3.1. Urban heat intensity through time for the entire study area, with maximum daily temperatures

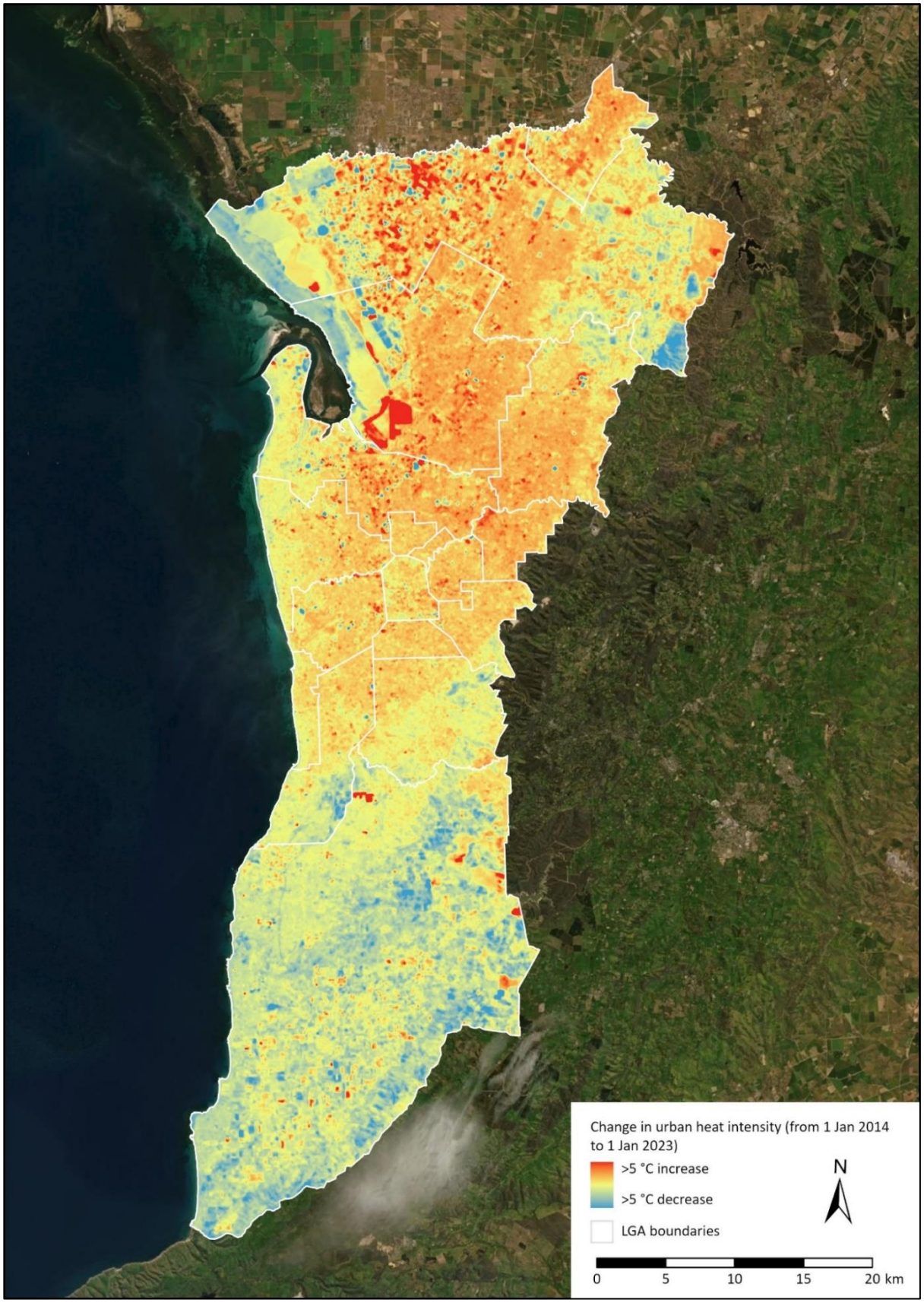

Figure 3.2. Trend results showing change in urban heat intensity (from 1 January 2014 to 1 January 2023) across the entire study area

Of the 18 LGAs in the study area, only one was classified as getting better, whereas 3 were classified as stable and the remaining 14 were classified as getting worse (Figure 3.3). The 3 LGAs with the greatest average increase in urban heat intensity of the time period were Campbelltown (1.9 °C increase), Gawler (1.6 °C increase) and Norwood Payneham & St Peters (1.6 °C increase).

As with the study area results, there are large variations of change in urban heat intensity within an individual LGA. For example, Playford and Salisbury both have large standard deviations, which are representative of the large range of change values within these areas.

Figure 3.4 maps the average change for each LGA and suburb and provides additional context of the variation within the study area. The suburb scale results show the increase in urban heat intensity particularly in the northern and north-eastern suburbs.

Refer to Appendix C for graphs of urban heat intensity through time for each LGA.

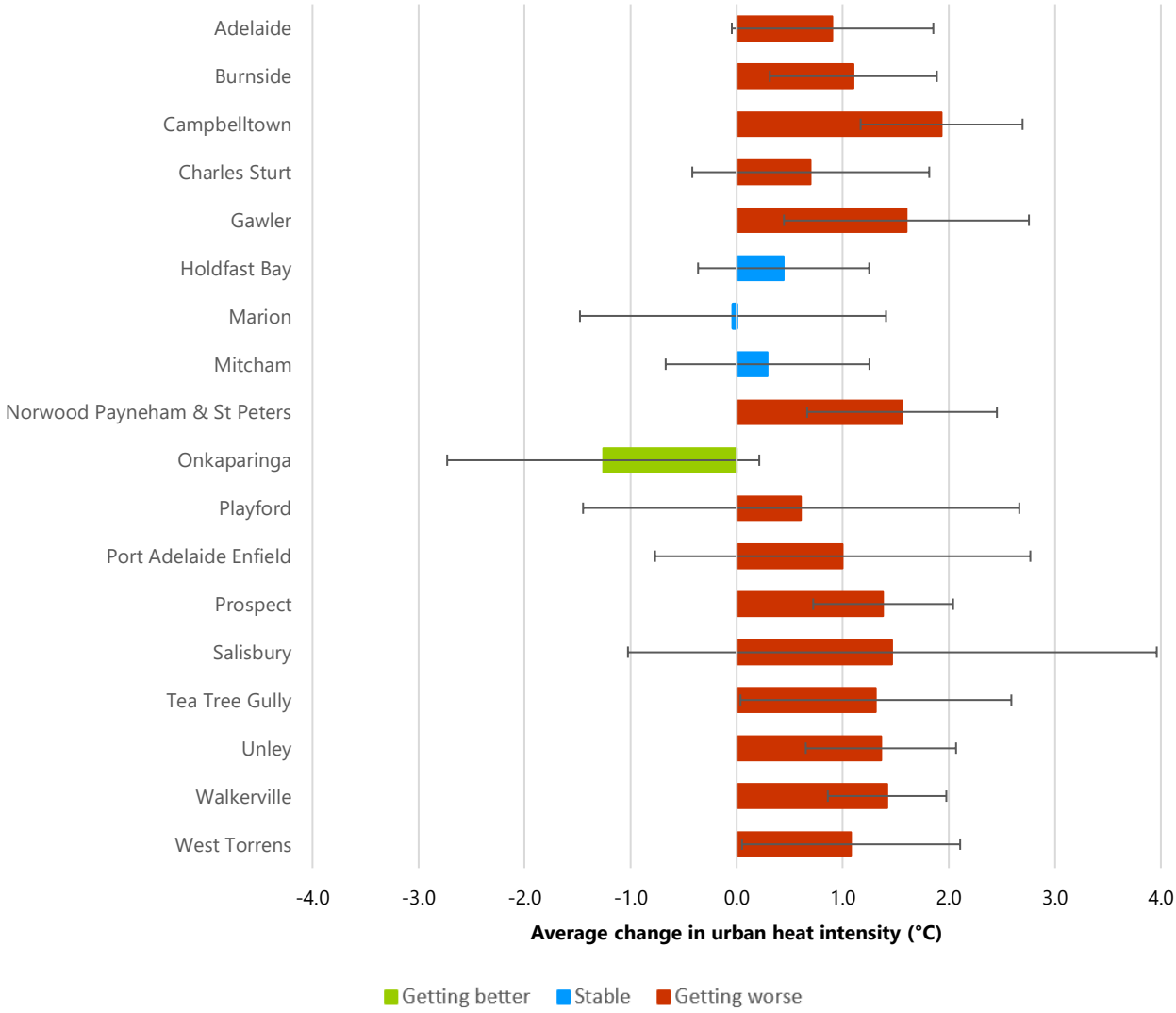

*Error bars are given as one standard deviation, and provide an indication of the spread of values within an LGA.

Figure 3.3. Trend results showing average change in urban heat intensity (from 1 January 2014 to 1 January 2023) for each LGA within the study area

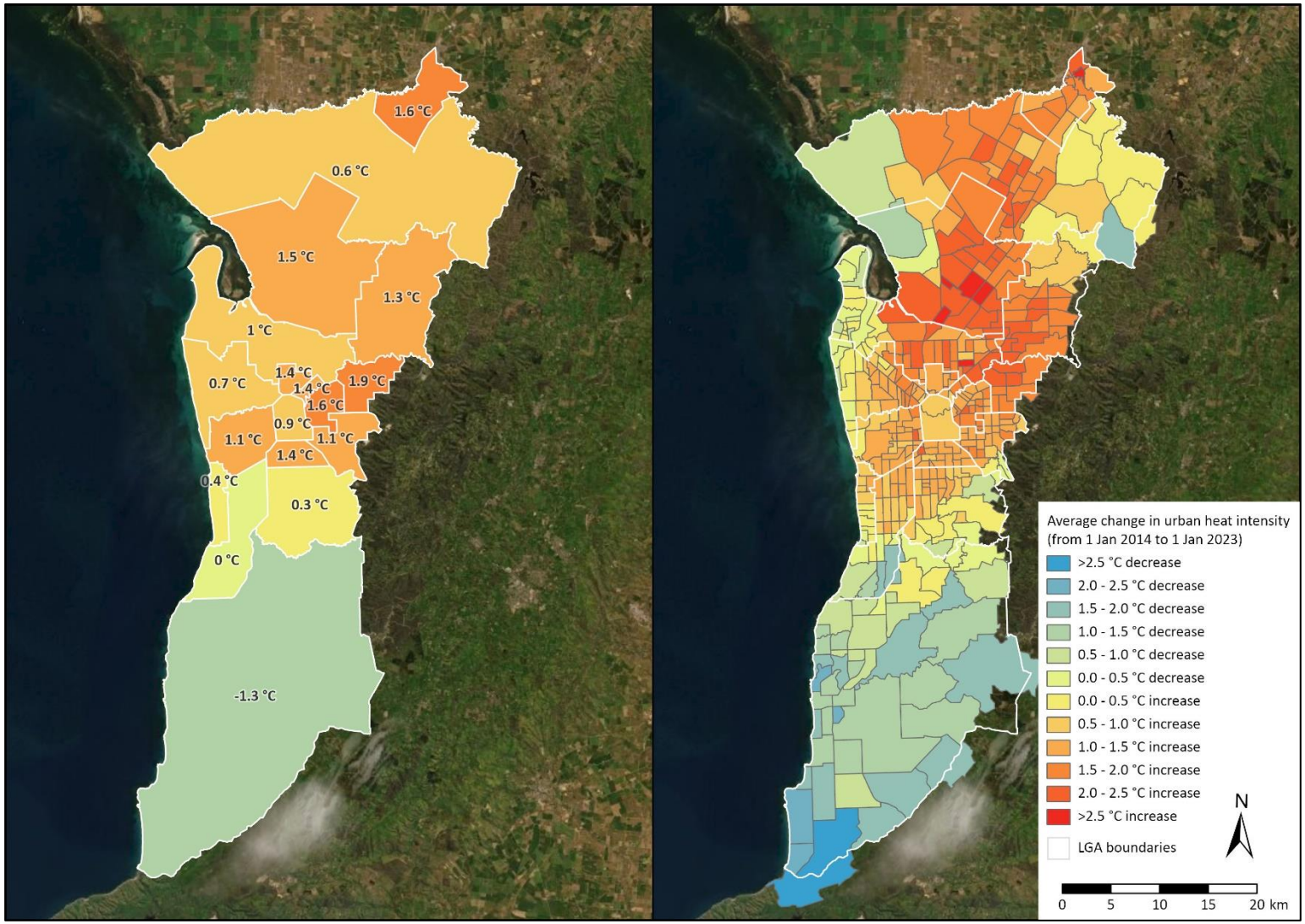

Figure 3.4. Trend results showing average change in urban heat intensity (from 1 January 2014 to 1 January 2023) for each LGA (left) and suburb (right) within the study area

3.2 Condition

Across the entire study area, the average urban heat intensity modelled for 1 January 2023 is 3.2 °C, that is to say, urban areas are on average 3.2 °C warmer compared to equivalent reference areas without any urban development. While the results indicate an overall fair condition, there is significant variation in temperature at the local scale within the study area driven by differences in surfaces (Figure 3.5). Temperature variations between surfaces is most evident for large homogenous areas consistent with the resolution of the Landsat imagery (100 m resolution), rather than heterogeneous areas where the resulting temperature is an average of all the mixed surfaces within the pixel.

For example, the surfaces with the lowest urban heat intensities within the study area are associated with water and dense vegetation, particularly mangroves. Whereas the highest urban heat intensities are associated with bare unirrigated surfaces and high-density urban areas with a greater prevalence of dark roofs and minimal green spaces.

Of the 18 LGAs in the study area, none were classified as very good, 3 were classified as good, 4 were classified as fair and the remaining 11 were classified as poor (Figure 3.6). The 3 LGAs with the greatest average urban heat intensity were Campbelltown (6.0 °C), Gawler (5.9 °C) and Norwood Payneham & St Peters (5.4 °C). The 3 LGAs with the lowest average urban heat intensity were Salisbury (1.8 °C), Mitcham (1.9 °C) and Charles Sturt (2.0 °C) (Figures 3.6 and 3.7).

As with the study area results, there are large variations of urban heat intensity within an individual LGA. For example, Salisbury, which is the coolest LGA is highly influenced by the cool mangroves and salt pans in the west of the LGA. This is also the case for Playford. The presence of open water in areas of Charles Sturt and Port Adelaide Enfield is also likely to have a cooling influence on the overall LGA's urban heat intensity. Conversely, the influence of hot dry paddocks in the peri-urban zone is strongly influencing the overall urban heat intensity of Onkaparinga.

Figure 3.7 shows the urban heat intensity for each suburb in the study area. The highest urban heat intensities are distributed around the southern peri-urban suburbs, as well as the northern and north-eastern suburbs. Cooler urban heat intensities are distributed in the north-west due to the presence of cool mangrove vegetation, as well as coastal suburbs and the south-eastern foothills.

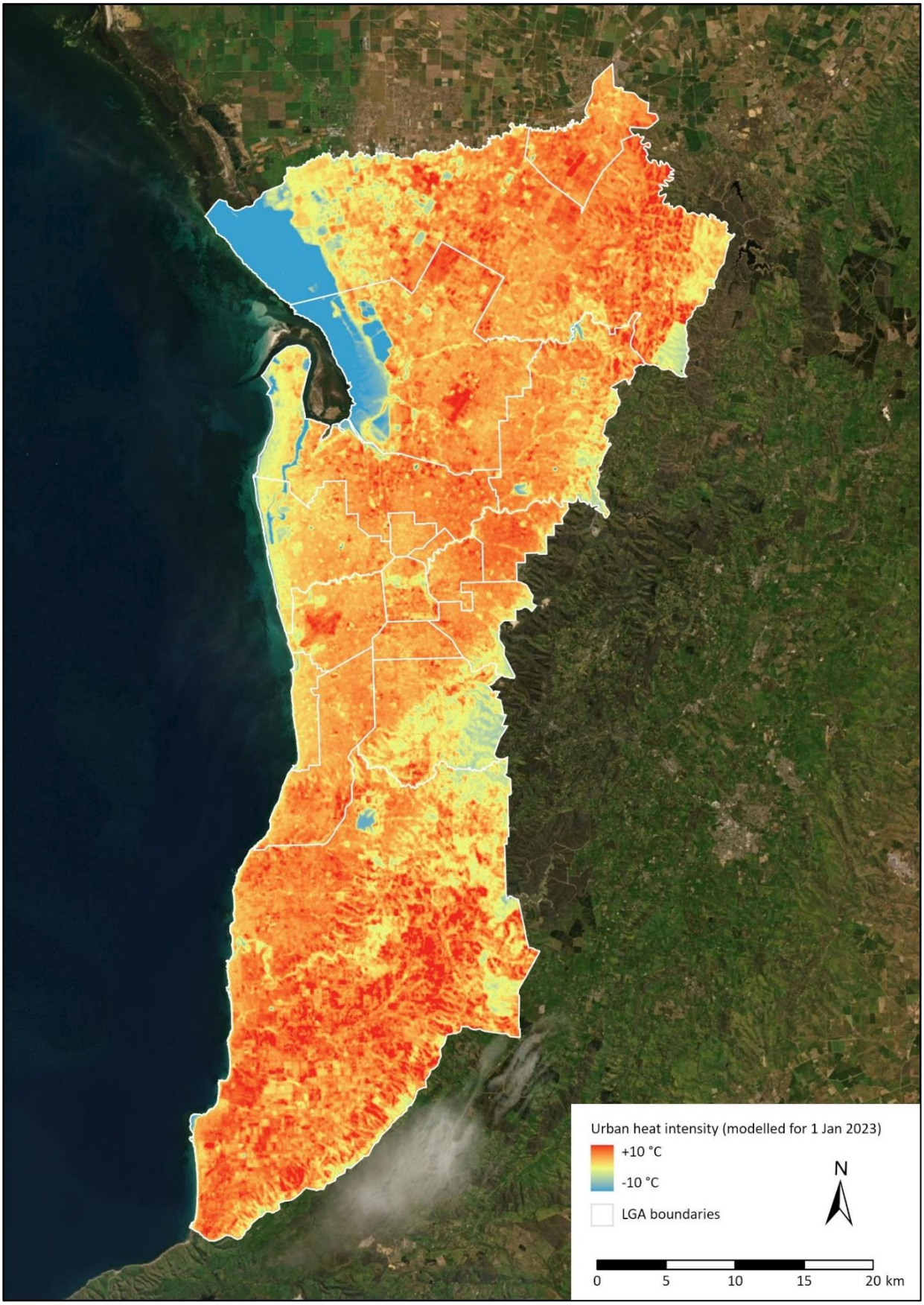

Figure 3.5. Condition results showing urban heat intensity (modelled for 1 January 2023) across the entire study area

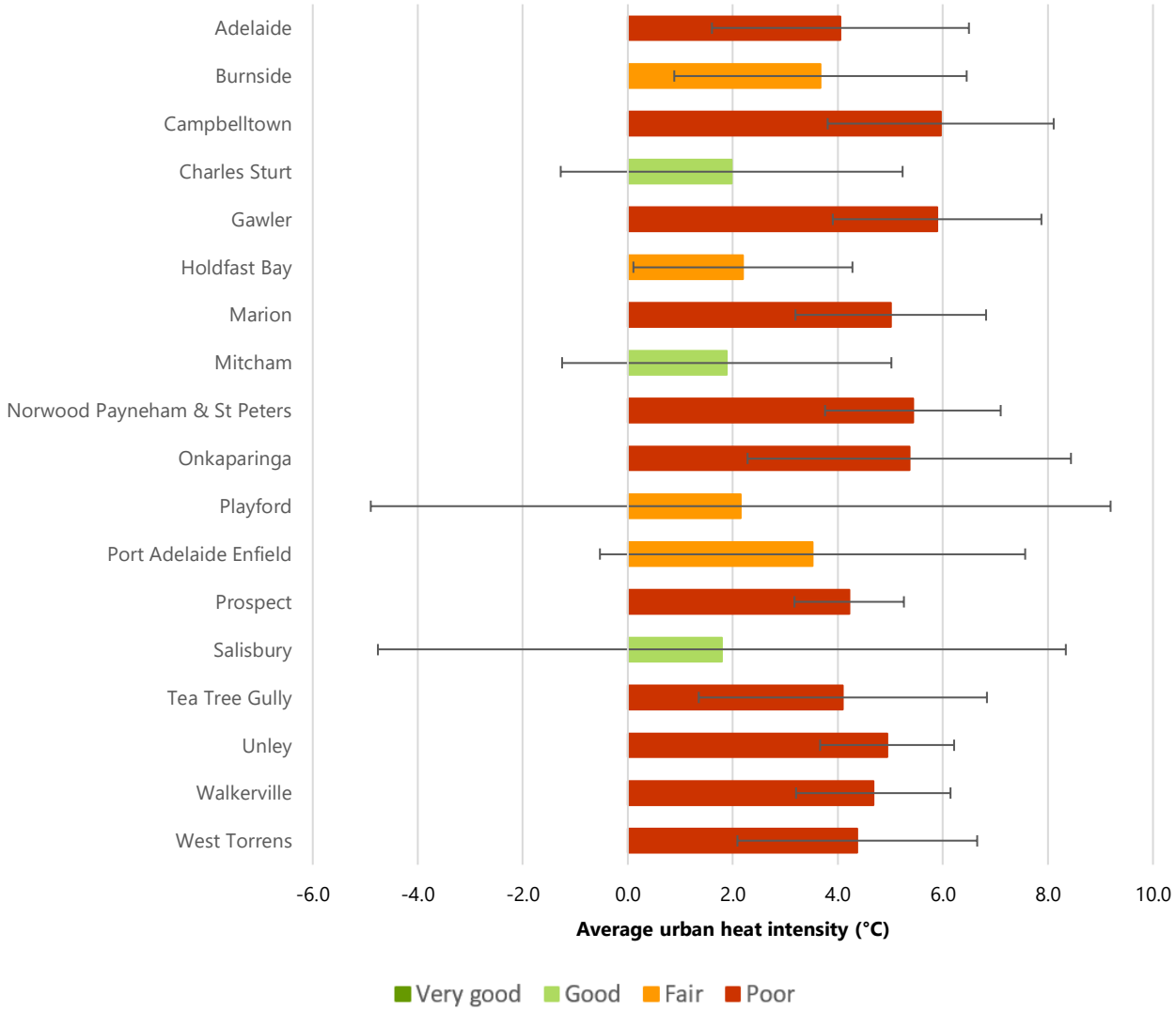

*Error bars are given as one standard deviation, and provide an indication of the spread of values within an LGA.

Figure 3.6. Condition results showing average urban heat intensity (modelled for 1 January 2023) for each LGA within the study area

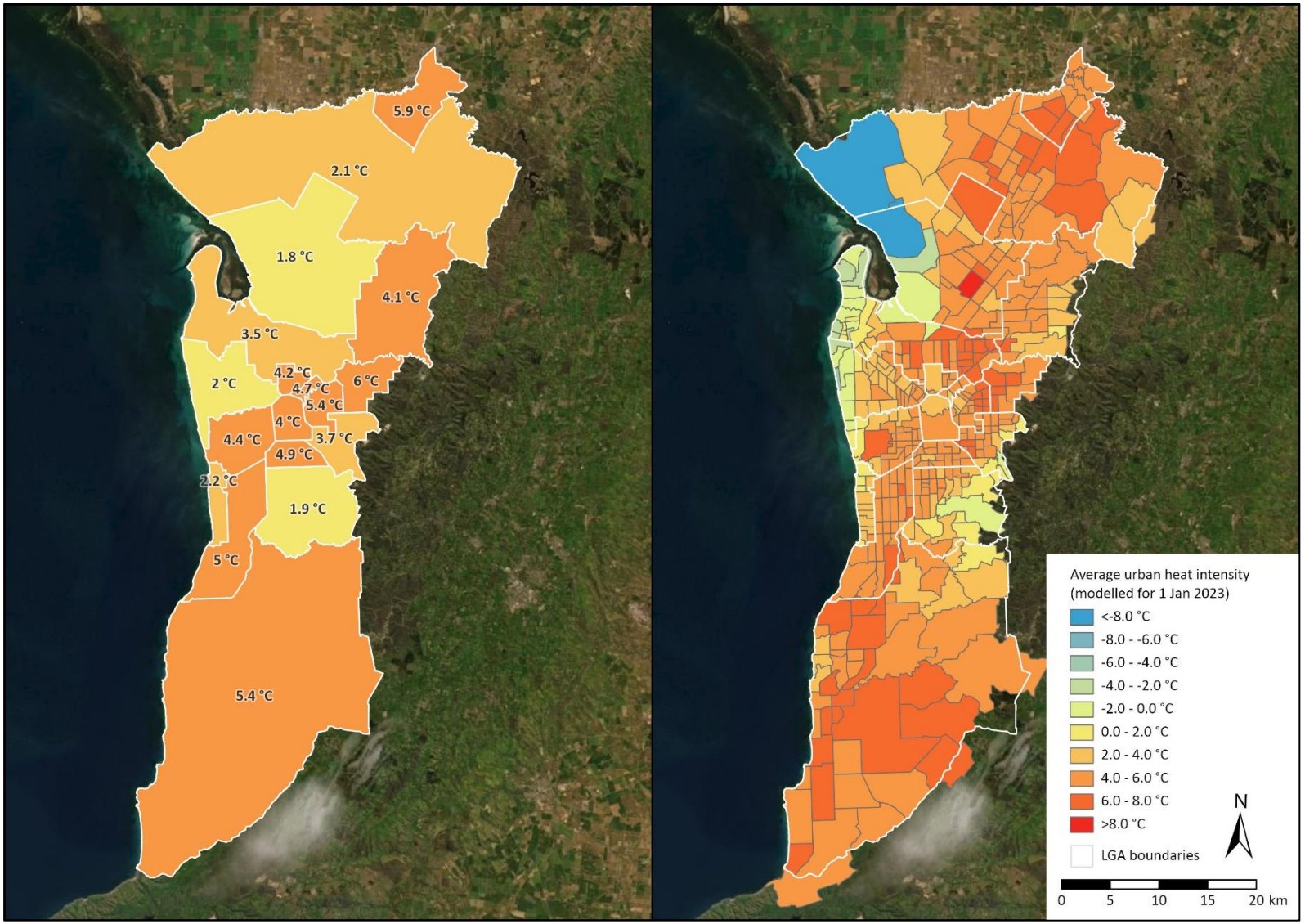

Figure 3.7. Condition results showing average urban heat intensity (modelled for 1 January 2023) for each LGA (left) and suburb (right) within the study area

3.3 Reliability

The overall reliability score for this report card is fair based on Table 3.1.

Table 3.1. Information reliability scores for urban heat

Indicator	Applicability	Currency	Spatial	Accuracy	Reliability
Urban heat intensity	2	5	5	2	2 (fair)

3.3.1 Notes on reliability

The report card has been given the score of 2 out of 5 and a reliability of fair based on the minimum score given for information currency, applicability, level of spatial representation and accuracy. This score was based on several considerations including:

- Applicability: the Landsat thermal sensor measures brightness temperature, which is measure of the amount of thermal infrared radiation emitted by the Earth's surface and atmosphere and is therefore an indirect measure of temperature. Brightness temperature is converted to surface temperature by the USGS as part of their processing prior to being delivered as a level-2 downloadable product.
- Currency: satellite imagery used in this analysis is based on Landsat data captured between December 2013 and January 2023, and is therefore current.
- Spatial: satellite imagery used in this analysis covers the entire study area.
- Accuracy: while this analysis is based on published methods, there are known limitations in generating the reference LST for an area which can impact the calculation of urban heat intensities. It is also difficult to quantitatively assess the accuracy of this data, therefore the accuracy is conservatively considered to be at least 60% better than could be expected by chance.

4 Discussion

4.1 Trend

The trend for urban heat across the Adelaide metropolitan area is stable, however at LGA scale the trend was variable. One LGA displayed a trend of getting better and three others were stable, and the remaining 14 LGAs displayed a trend of getting worse (Figure 3.3). The LGAs in the southern portion of the study area displaying either cooling or stable trends account for approximately 40% of the total metropolitan area. This likely contributed to the overall stable trend in urban heat.

When average change in urban heat is observed at LGA and suburb scale, local patterns of variability are observed (Figure 3.4). Suburbs in the inner south and west, and in the north and north-east are displaying a trend of warming, whereas the peri-urban areas of Onkaparinga and the eastern and western extents of Playford are experiencing cooling. Local effects such as changes to surface types, ratio of vegetation to bare ground or built surfaces, and presence or absence of water bodies influence the variability of temperatures observed across LGAs and across the region.

4.2 Condition

As there is no established method for assigning condition thresholds, condition was assigned based on the range of urban heat intensity values observed in this survey (Table 2.3). Urban areas across metropolitan Adelaide are on average 3.2 °C warmer compared to equivalent reference areas without any urban development. For the purpose of this study the condition was rated as fair, relative to the range of temperatures observed. As reflected in the error margins however, there is significant variability in the intensity of urban heat across the region.

Urban heat across the Adelaide metropolitan area is highly spatially variable due to patterns in the built environment, land use and land cover types, and presence or absence of vegetation, including street trees, parks and gardens.

At a local scale, patterns in urban heat reflect the underlying surface types. Areas with a high proportion of vegetation or surface water are cooler than areas with a high proportion of bare dry land, and hard, impermeable surfaces such as roads and buildings.

At LGA scales, patterns of urban heat reflect the larger trends of neighbourhood composition. Areas with a high proportion of housing, industrial infrastructure or both tend to display higher urban heat than areas with a high proportion of vegetation or lower density housing. This is reflected particularly in the variability observed in Salisbury, which has a condition rating of good (1.8 °C), where the western extents are influenced by the cooling effects of the coastal mangroves and in the east by the heavily urbanised landscape.

5 Appendices

A. Change in summer land surface temperature for Perth

Environmental consultants, Astron, presented the findings of their study into change in LST across the Perth metropolitan area as a poster at the Advancing Earth Observation Forum in Brisbane in August 2022 (Kovacs-Ledo and Archibald 2022). The following figure is a snapshot of this analysis shared online (https://bit.ly/3ll9z0d, accessed 21/11/2022).

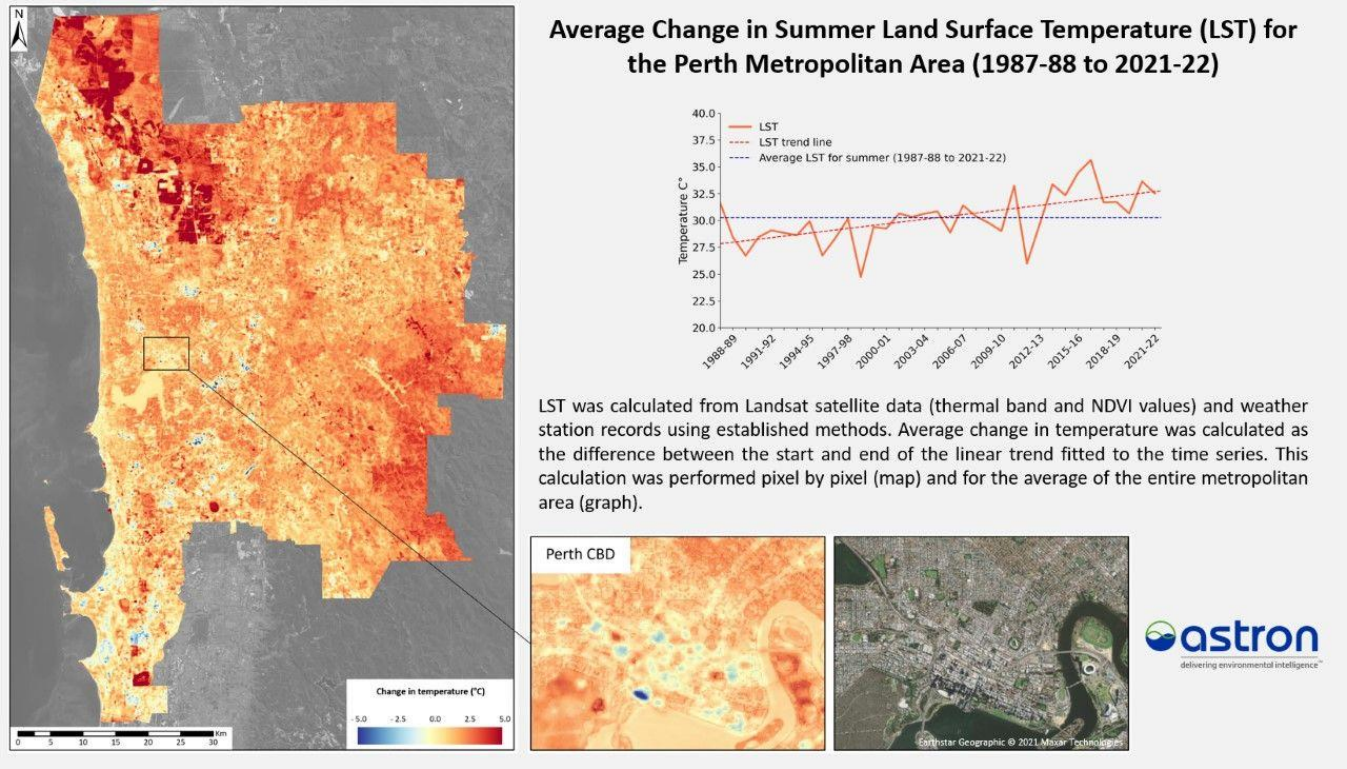

B. Managing environmental knowledge chart for urban heat

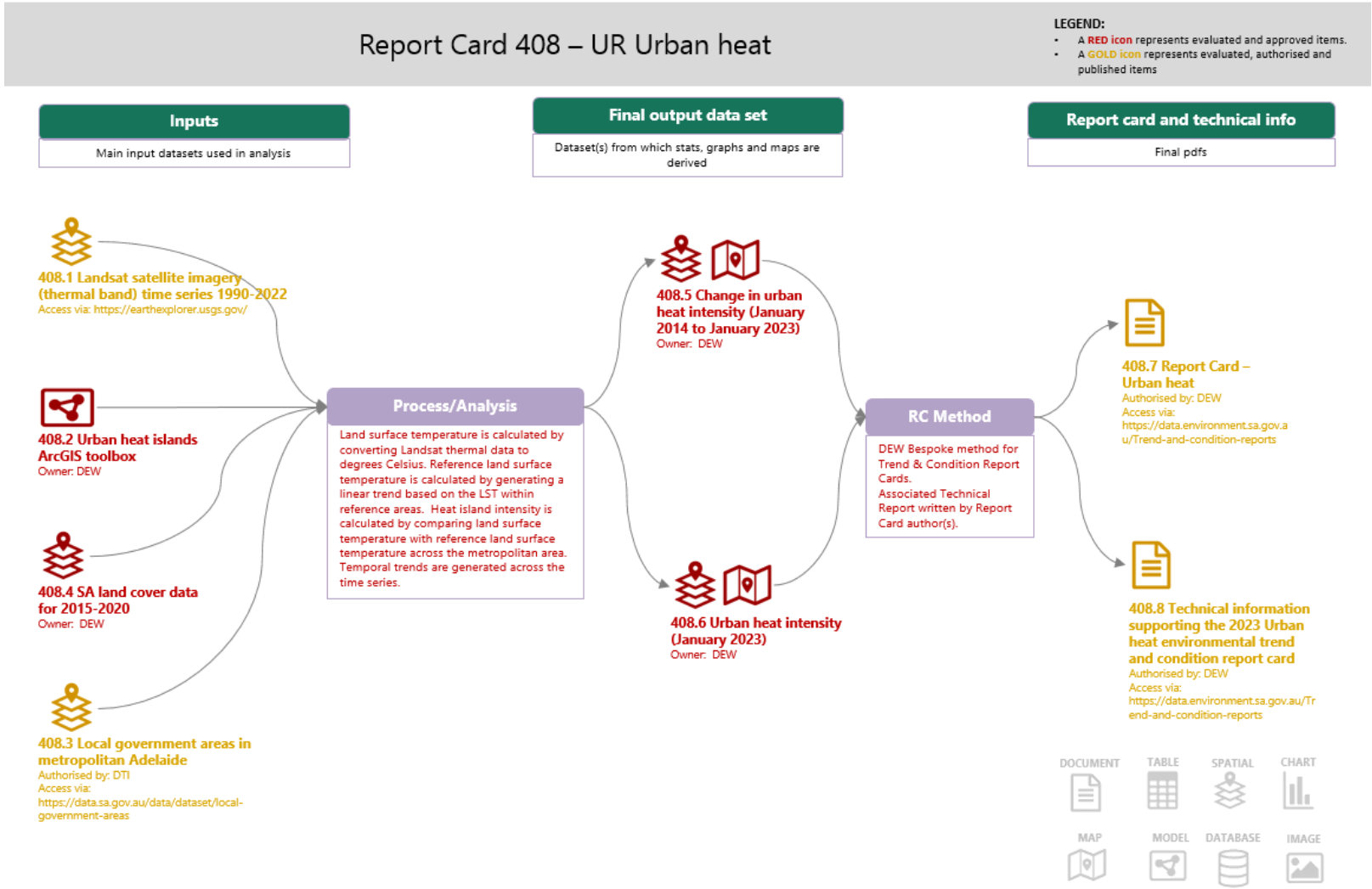

C. Urban heat intensity through time for each LGA within the study area

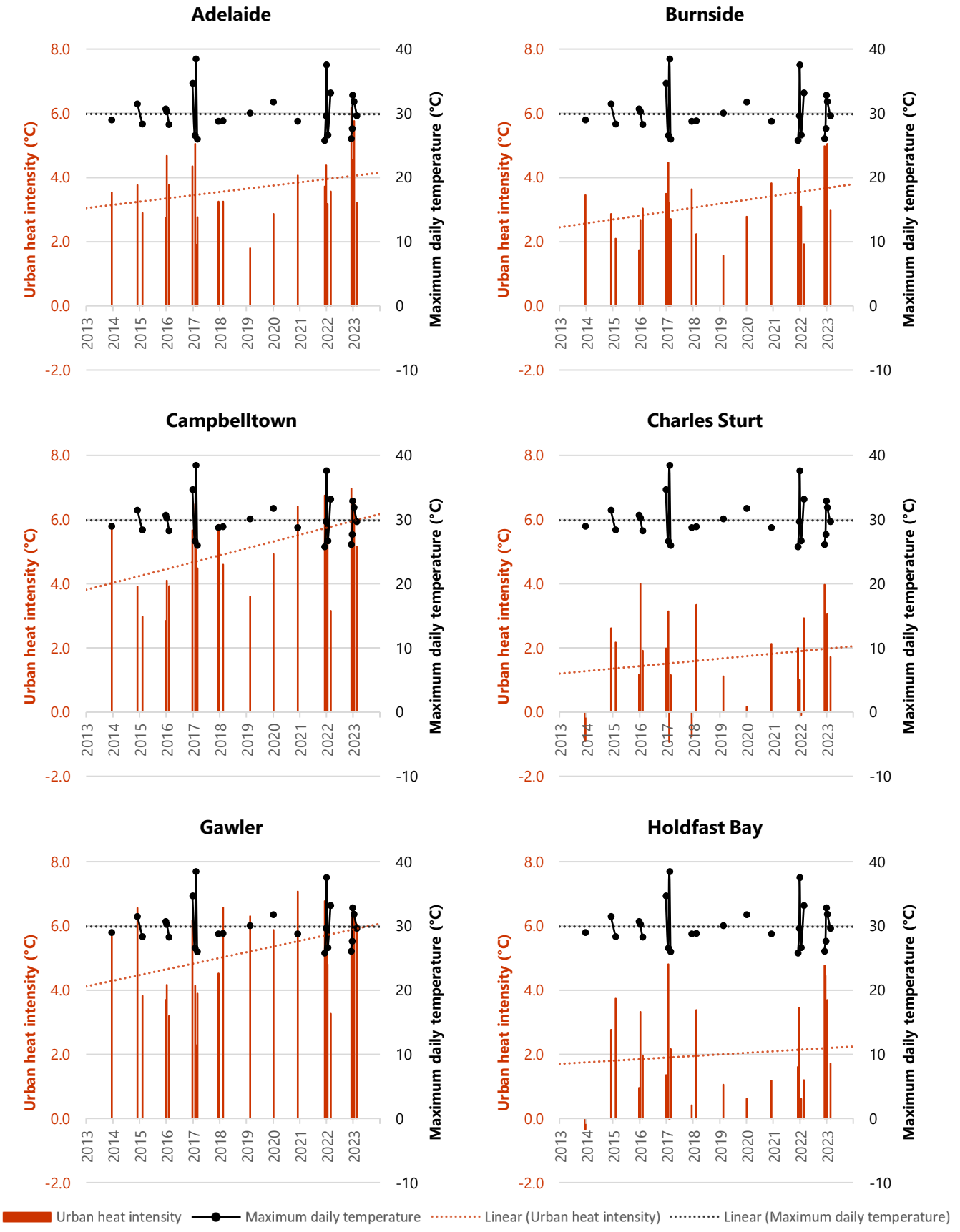

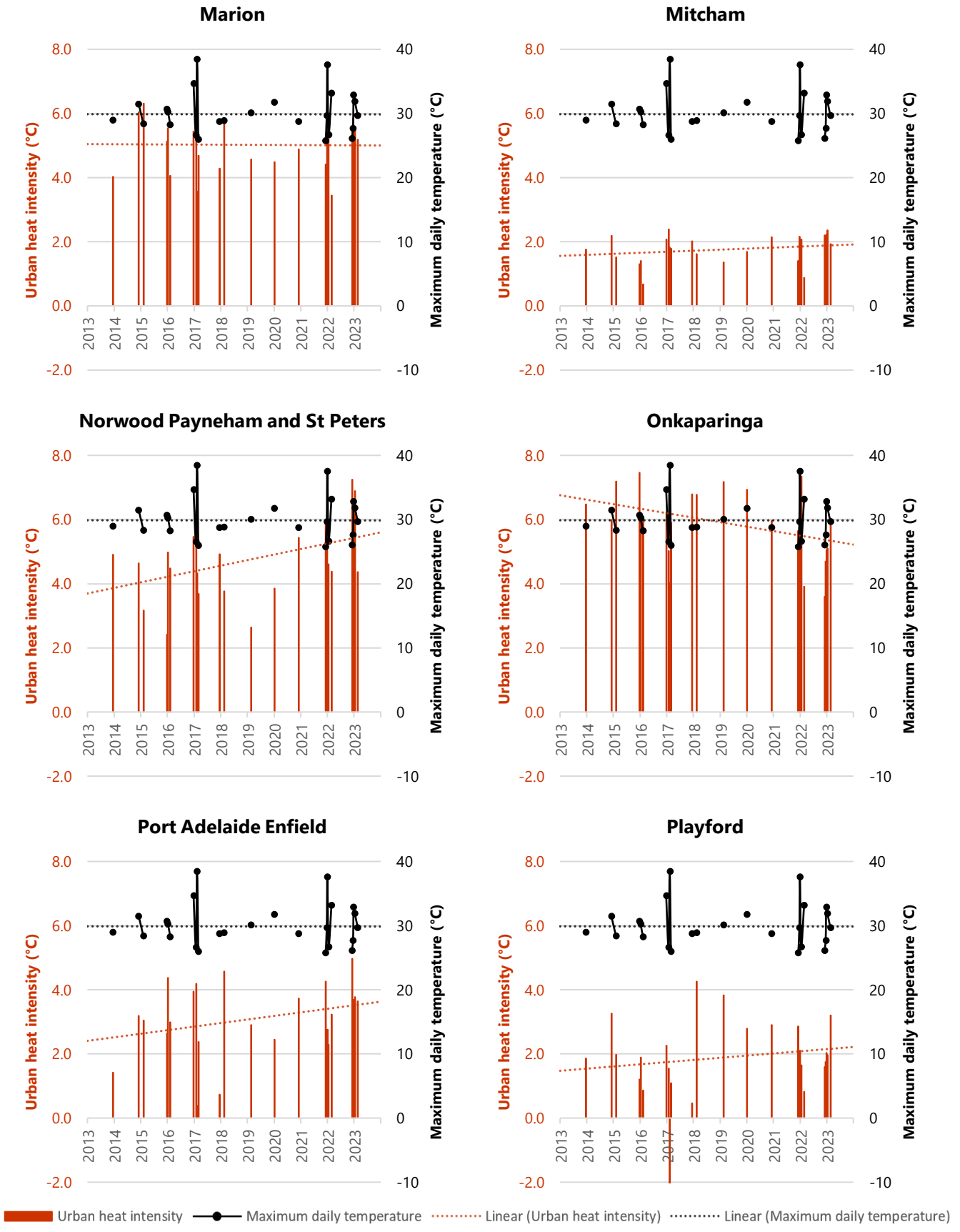
Marion
Mitcham
Norwood Payneham and St Peters
Onkaparinga
Port Adelaide Enfield
Playford
Urban heat intensity (°C)
Maximum daily temperature (°C)
8.0
6.0
4.0
2.0
0.0
-2.0
40
30
20
10
0
-10
2013
2014
2015
2016
2017
2018
2019
2020
2021
2022
2023
Urban heat intensity
Maximum daily temperature
Linear (Urban heat intensity)
Linear (Maximum daily temperature)

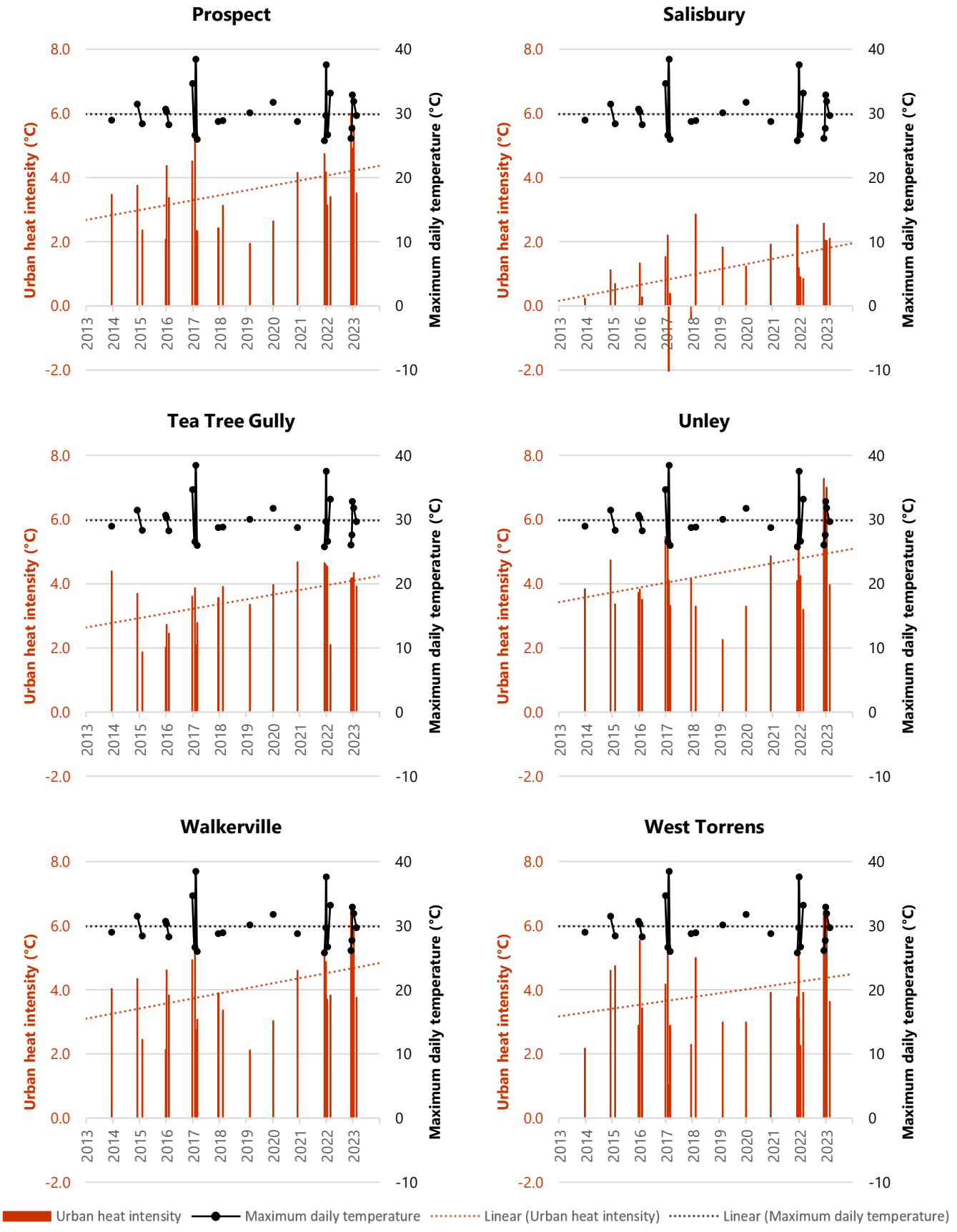
Prospect
Salisbury
Tea Tree Gully
Unley
Walkerville
West Torrens
Urban heat intensity (°C)
Maximum daily temperature (°C)
8.0
6.0
4.0
2.0
0.0
-2.0
40
30
20
10
0
-10
2013
2014
2015
2016
2017
2018
2019
2020
2021
2022
2023
Urban heat intensity
Maximum daily temperature
Linear (Urban heat intensity)
Linear (Maximum daily temperature)

6 References

Adapt NSW (2023). Climate change impacts on urban heat. https://www.climatechange.environment.nsw.gov.au/urban-heat (accessed 28/2/2023).

Bartesaghi-Koc C, Soebarto V, Hawken S & Sharifi E (2022). The potential for urban canopy cover to reduce heat-related mortality, In: Urban Overheating: Heat Mitigation and the Impact on Health (eds N. Aghamohammadi, M. Santamouris), pp. 249-273, Springer Nature Singapore Pte Ltd.

Devereux D & Caccetta P (2017). Estimation of land surface temperature and urban heat island effect for Australian urban centres, Report EP173542 for Horticulture Innovation Australia (HIA) *Where Should All the Trees Go?* Project, CSIRO Data 61, Australia.

Jain S, Sannigrahi S, Sen S, Bhatt S, Chakraborti S & Rahmat S (2020). Urban heat island intensity and its mitigation strategies in the fast-growing urban area, Journal of Urban Management, 9, 54-66.

Kovacs-Ledo T & Archibald R (2022). Perth is no longer cool – monitoring and managing urban temperatures using remote sensing, Advancing Earth Observation Forum, August 2022, Brisbane, Australia, https://static1.squarespace.com/static/6061336899931c5e384e5946/t/63803f534a02e4169a293379/1669349211322/AEO2022%2BAbstracts.pdf (accessed 17/3/2023).

Norton BA, Coutts AM, Livesley SJ, Harris RJ, Hunter AM & Williams NSG (2015). Planning for cooler cities: A framework to prioritise green infrastructure to mitigate high temperatures in urban landscapes, Landscape and Urban Planning, 134, 127-138.

Physical Environment Research Network (2021). Reducing Illness and Lives Lost from Heatwaves: Project Report. Canberra, Australia: Australian Government Data Integration Partnership for Australia. https://www.pean.gov.au/projects/heatwaves-and-health

Shukla PR, Skea J, Buendia EC, Masson-Delmotte V, Pörtner HO, Roberts DC, Zhai P, Slade R, Connors S, van Diemen R, Ferrat M, Haughey E, Luz S, Neogi S, Pathak M, Petzold J, Portugal Pereira J, Vyas P, Huntley E, Kissick K, Belkacemi M & Malley J (2019). Technical Summary, 2019. In: Climate Change and Land: an IPCC special report on climate change, desertification, land degradation, sustainable land management, food security, and greenhouse gas fluxes in terrestrial ecosystems (eds PR Shukla, J Skea, R Slade, R van Diemen, E Haughey, J Malley, M Pathak, J Portugal Pereira), https://doi.org/10.1017/9781009157988.002.

USGS (2021). Landsat 8-9 Calibration and Validation (Cal/Val) Algorithm Description Document (ADD) Version 4.0 January 2021, Department of the Interior, U.S. Geological Survey, Sioux Falls, South Dakota.

USGS (2022). Landsat 8-9 Collection 2 (C2) Level 2 Science Product (L2SP) Guide Version 4.0 March 2022, Department of the Interior, U.S. Geological Survey, Sioux Falls, South Dakota.

Voogt, JA (2008). How researchers measure urban heat islands, University of Western Ontario, London, Ontario, Canada, https://www.researchgate.net/publication/237288704_How_Researchers_Measure_Urban_Heat_Islands (accessed 14/3/2023).

Wai CY, Muttil N, Tariq MAUR, Paresi P, Nnachi RC & Ng AMW (2022). Investigating the relationship between human activity and the urban heat island effect in Melbourne and four other international cities impacted by COVID-19, Sustainability, 14, 378, https://doi.org/10.3390/su14010378.

Zhou D, Xiao J, Bonafoni S, Berger C, Deilami K, Zhou Y, Frolking S, Yao R, Qiao Z & Sobrino JA (2019). Satellite remote sensing of surface urban heat islands: progress, challenges, and perspectives, Remote Sensing, 11(1), 48, https://doi.org/10.3390/rs11010048.

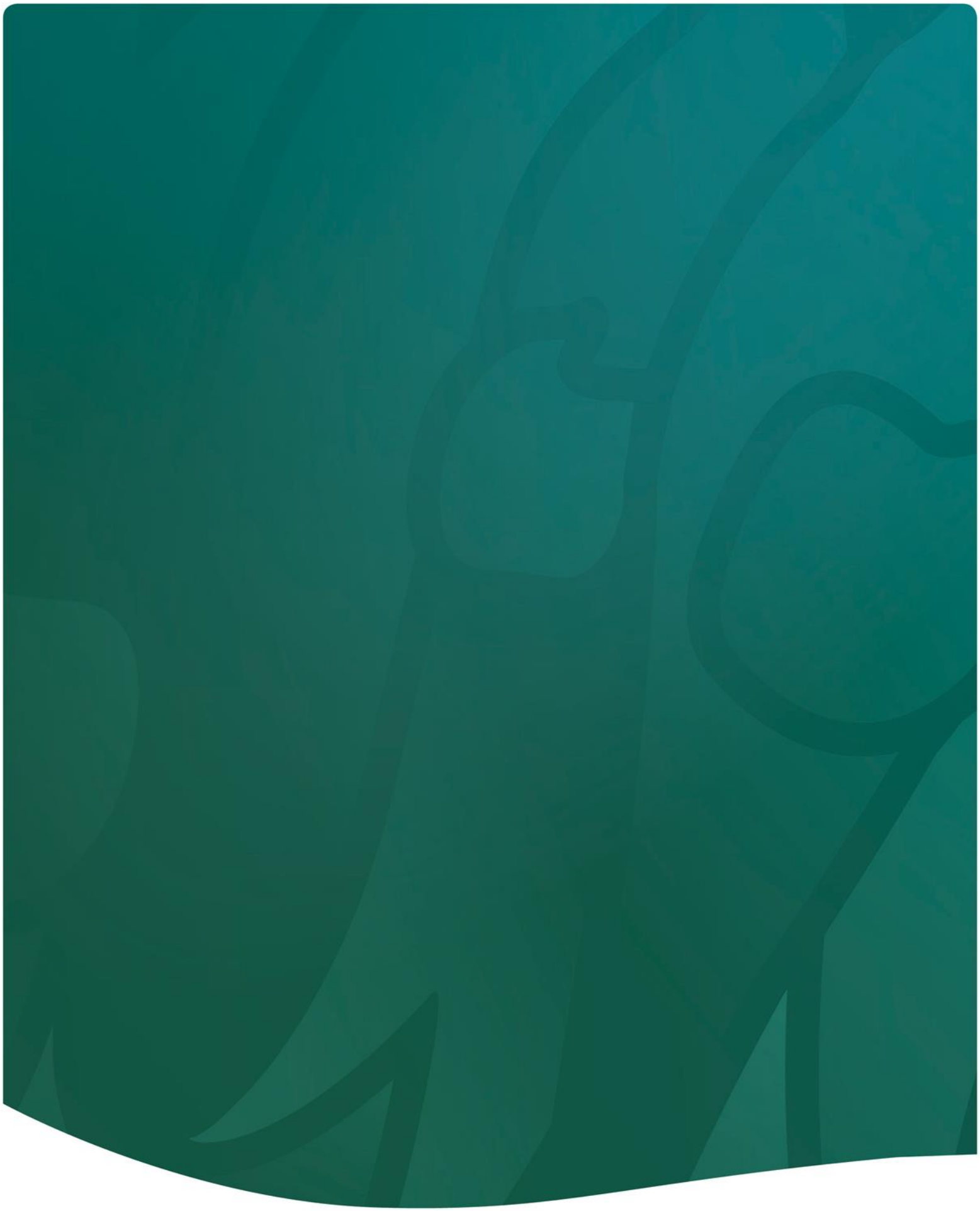

Government
of South Australia

Department for
Environment and Water